Available online at www.sciencedirect.com
ScienceDirect
Earth and Planetary Science Letters 251 (2006) 134–147
EPSL
www.elsevier.com/locate/epsl

Riverine behaviour of uranium and lithium isotopes in an actively glaciated basaltic terrain

Philip A.E. Pogge von Strandmann [a,*], Kevin W. Burton [a], Rachael H. James [a], Peter van Calsteren [a], Sigurður R. Gíslason [b], Fatima Mokadem [a]

[a] *Department of Earth Sciences, CEPSAR, The Open University, Milton Keynes, MK7 6AA, UK*
[b] *Institute of Earth Sciences, University of Iceland, Reykjavik, Iceland*

Received 20 February 2006; received in revised form 22 August 2006; accepted 1 September 2006
Available online 12 October 2006
Editor: H. Elderfield

Abstract

This study presents U and Li isotope and major and trace element data for the dissolved load, suspended particulates and bedload for Icelandic rivers draining predominantly basaltic catchments. Physical erosion rates range from 920 to 2084 t/km^2/yr, with the higher values associated with glacier-fed rivers. Chemical erosion rates range from 45 to 91 t/km^2/yr, with lower rates being associated with glacier-fed rivers. Uranium activity ratios, (^{234}U/^{238}U), are close to secular equilibrium in the suspended and bedloads, but all dissolved load samples show values greater than unity, ranging from 1.13 to 2.41. The highest (^{234}U/^{238}U) values are found in glacier-fed rivers, and can be attributed to α-recoil effects, as grinding by glaciers locally enhances rates of physical weathering. Activity ratios in glacial rivers decrease with distance from the glacial source due to input from non-glacial tributaries which have high levels of dissolved uranium and lower activity ratios. In contrast, in non-glacial rivers, uranium activity ratios increase with distance downstream due to continued weathering in soils and of bedrock. The δ^7Li value of the suspended load is always lower than that of the bedload due to preferential retention of ^{6}Li in secondary minerals during weathering. In turn, the δ^7Li value of the dissolved load is always greater than that of the bedload, ranging from 17.0 to 43.7‰. δ^7Li for the dissolved load decreases with increasing levels of dissolved silicon, and the saturation index of secondary minerals, which suggests that δ^7Li decreases with increasing chemical weathering. There is no correlation between δ^7Li values and uranium activity ratios for the dissolved load for non-glacial rivers, but for glacier-fed rivers there is an increase in δ^7Li with increasing (^{234}U/^{238}U), suggesting that where physical comminution of mineral grains by glaciers is high, chemical weathering is suppressed, and vice-versa.

Keywords: uranium isotopes; lithium isotopes; basalt weathering; glacial weathering; iceland

1. Introduction

Chemical weathering of Ca–Mg silicates exerts a control on global climate, through its effect on atmospheric CO_2 levels, which in turn can drive temperature changes by modifying greenhouse warming (e.g. [1–3]). Amongst silicate rock types, basalts are highly susceptible to weathering, and thus have a much greater effect on atmospheric CO_2 consumption than might be expected from their areal extent [4,5]. For example, estimates for present-day CO_2 consumption due to silicate weathering suggest that around 35% may be

* Corresponding author. Fax: +44 1908 655151.
E-mail address: P.PoggevonStrandmann@bristol.ac.uk (P.A.E. Pogge von Strandmann).

0012-821X/$ - see front matter © 2006 Elsevier B.V. All rights reserved.
doi:10.1016/j.epsl.2006.09.001

attributable to basaltic rocks, even though they constitute less than 5% of the continental area [1].

In principle, a number of radiogenic isotope ratios in seawater are sensitive to changes in the balance of input from silicate weathering, and temporal variations can often be linked to climatic and tectonic events (e.g. [6]). However, changes in silicate weathering rates are difficult to distinguish from changes caused by variations in source, such as rock type and age, geographical location or even the weathering process itself. Application of uranium-series disequilibria circumvents the problem of compositional variations because secular equilibrium can be assumed for all rocks older than ca. 1 Ma, giving an activity ratio equal to one. Energetic alpha decay of ^{238}U results in the preferential release of ^{234}U due to α-recoil effects, and high $^{234}U/^{238}U$ ratios are normally found in surface waters draining catchments with high physical weathering rates, such as glaciated terrains where physical comminution of grains is likely to be significant. In contrast, in regions of high rainfall, and hence runoff, recoil ^{234}U is rapidly removed (e.g. [7–10]). The stable isotopes of lithium (Li), ^{6}Li and ^{7}Li, are fractionated during weathering, and such fractionation is also largely independent of rock type [11]. Both field and experimental studies have shown that ^{6}Li is preferentially retained by secondary weathering minerals during silicate weathering [12–16]. Accordingly, the fractionation of Li isotopes is dependent upon the extent of chemical weathering. Large fractionation seems to occur during superficial weathering in high-relief areas while little fractionation is observed during more intense or prolonged weathering in stable environments [12,15].

Iceland provides the opportunity to study the effects of weathering and glacial erosion processes on more or less uniform basaltic lithologies, at a relatively constant average temperature and relatively simple vegetative cover, but with variable rainfall (and river discharge), rock age, and glacial cover. Younger basalt terrains experience high physical and chemical erosion rates, partly due to the high runoff associated with active glaciation, but also due to the high abundance of basaltic glass, produced during sub-glacial eruptions, which dissolves much faster than crystalline basalt [5,17–19]. Glacial cover increases the pH of waters by excluding atmospheric CO_2 [20], which decreases the dissolution rate of Ca–Mg silicates [21–23], but increases the dissolution rate of Al-silicates like basaltic glass and plagioclase [24,25]. At high pH levels primary Ca–Mg silicates [26,27] and some secondary weathering minerals [19] are relatively stable. In contrast, the older basalt terrains experience lower erosion rates and runoff. The pH of waters on the older terrains tends to be lower partly because of higher surface runoff relative to groundwater flow and lesser amounts of basaltic glass, but also because of higher levels of vegetation cover. Thus, the primary basaltic minerals are less stable, and the stability of secondary weathering products is variable.

This study presents comprehensive elemental concentration and U and Li isotope data for river systems in western and southern Iceland. These results illustrate the relationship of riverine U and Li isotope ratios with physical and chemical erosion rates, the weathering of primary basalt phases, and the precipitation of secondary minerals.

2. Geology, climate and river setting

Iceland is geologically young, formed of predominantly (80–85%) basaltic rocks [5] within the last 25 Ma, although the oldest rocks exposed at the surface are no older than 14 Ma [28]. Recent and Upper Quaternary rocks are mainly confined to the active volcanic zones, which follow the SW–NE trend of the mid-Atlantic ridge.

The climate in Iceland is oceanic boreal, with a mean annual temperature of 4 °C around Reykjavik in the SW of the island. Mean annual precipitation is ~3000 mm on the south coast, ~1000 mm on the west coast and less than 400 mm in the central highlands. Roughly 11% of the island's 103,000 km^2 is glaciated, dominantly by four major icecaps, which reached their current size about 8000 yr ago [29]. Three types of rivers exist in Iceland: spring-fed rivers, which are mainly located in the active volcanic zones, glacier-fed rivers and direct runoff rivers. The latter mostly drain the older basaltic areas, due to a decrease in rock permeability with rock age. This is because in the older rocks compaction and sealing by secondary minerals reduces the permeability by up to five orders of magnitude [30].

The mean physical (mechanical) erosion rate of Icelandic rivers is about 500 $t/km^2/yr$ [31], which is almost three times the world average for physical denudation [32]. The mean chemical erosion rate of rock derived elements is about 55 $t/km^2/yr$ for Southwest Iceland, and 37 $t/km^2/yr$ for all of Iceland [33], although locally this has been shown to be inhibited by glacial cover [5].

Here two areas of Iceland have been studied in detail. Each is dominantly basaltic, but each possesses different bedrock age, glacial and vegetative cover, and each is affected by differing physical and chemical erosion rates. The first area is a river catchment which drains into the Borgarfjörður estuary, in the west of Iceland (Fig. 1). The average age of the bedrock in this catchment is

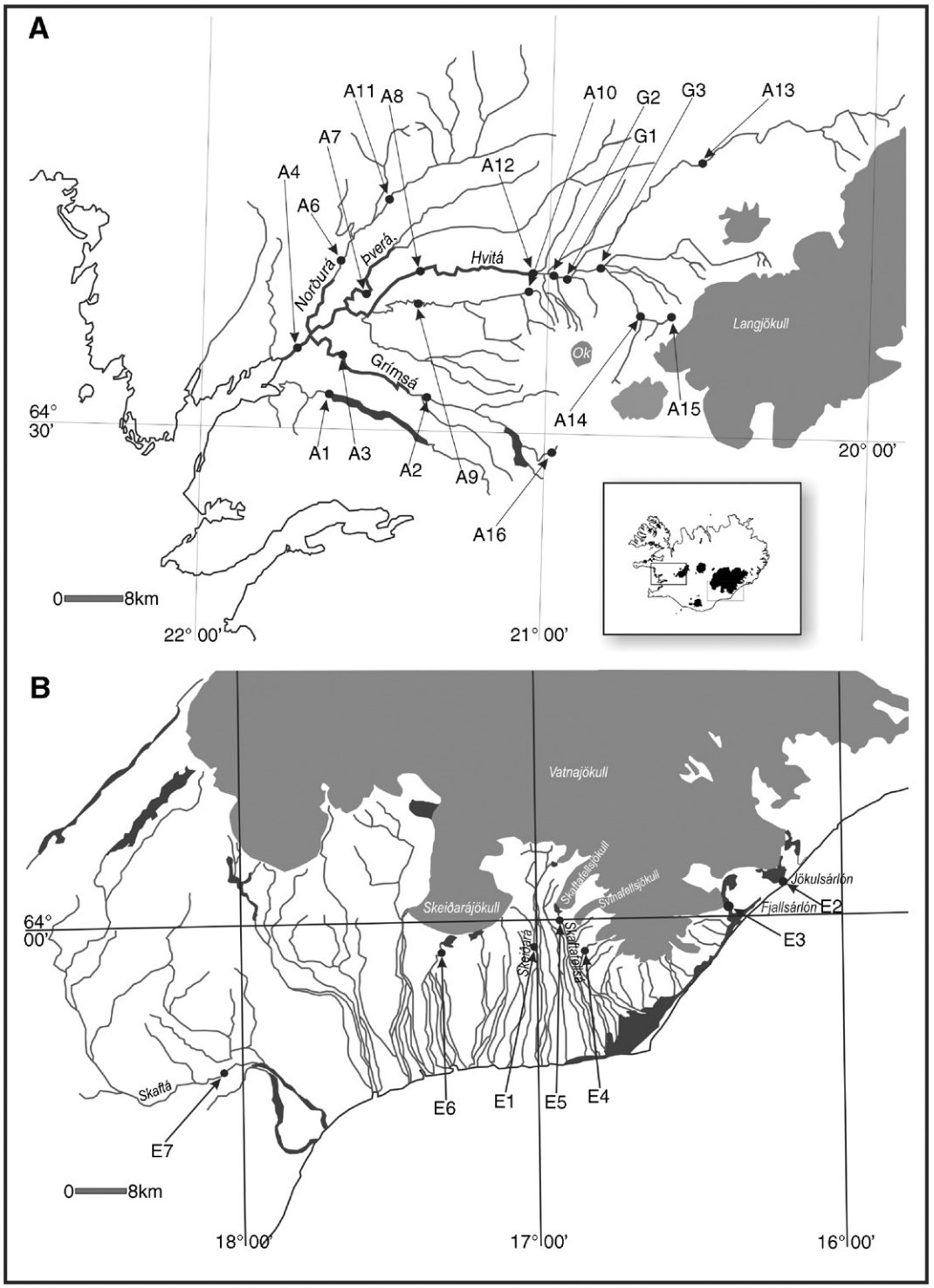

Fig. 1. Sample localities in western (A) and southeastern (B) Iceland.

Tertiary (>3.1 Ma) and 18 samples were taken from both the main Hvítá River, which is fed by the Langjökull icecap, and the major (non-glacial) tributaries (Fig. 1A). This includes a groundwater sample taken from the Hraunfossar falls, where water flows into the Hvítá from between layers of the tenth century Hallmundarhraun

lava field. Hot spring samples (Deildartunguhver) and ice samples (from Langjökull) were also collected to assess the impact of hydrothermal water and atmospheric precipitation on river chemistry. The lower areas of this catchment have been studied previously [5] and element concentrations, mineral saturation states and weathering rates were ascertained. The second area is in the south east of Iceland and comprises 7 rivers running off from the south of the Vatnajökull icecap (Fig. 1B), including the Jökulsárlón glacial lagoon, in which bedrock ages range from Quaternary to Recent.

3. Field and analytical techniques

3.1. Sampling

Samples were collected in September 2003 and August 2005. In the field, rivers were sampled from the centre of the flow (often from bridges). Water was collected in pre-cleaned containers, and where possible bedload was also collected. At each site pH, temperature, alkalinity, conductivity and total suspended sediment (TSS) were also measured. Each water sample was filtered, on the day of collection, through 0.2-μm cellulose acetate filters using a pressurised teflon unit, and whenever possible suspended particulate material was recovered from the acetate filters.

3.2. Cations, anions and trace elements

Bedload sands and suspended particulate material were finely powdered and dissolved in $HF–HNO_3$. Major element concentrations for the bedload were measured by X-ray fluorescence (XRF) with a 2σ external uncertainty better than 1%. Cation concentrations in the suspended and dissolved loads were measured by inductively coupled plasma mass spectrometry (ICP-MS). Major elements were calibrated against a set of synthetic multi-element standards prepared gravimetrically from high purity single element standard solutions. The accuracy of the analysis was assessed by running the natural water certified reference material SLRS-4. The following certified reference materials were used for external calibration: BHVO-2, BIR-1, JB-2, BCR-2. BHVO-2 was used as a monitoring standard for each batch of measurements. The 2σ external uncertainty for these measurements is better than ±3.2% for major elements and ±5% for trace elements. The major anion concentrations in the dissolved load were measured by ion chromatography, with an uncertainty better than ±4% for all anions.

3.3. U and Li isotopes

For the U-isotope ratios, 200 ml of filtered water were evaporated after spike addition, and then passed through cation exchange resin. Measurements were made by thermal ionisation mass spectrometry (TIMS) on single Re filaments, with a 2σ external error of ±0.056 on the ($^{234}U/^{238}U$) activity ratio (where parentheses denote activity ratio), using a diluted (25 ng/l), spiked NIST U960 standard. U concentrations were also measured in all samples by isotope dilution, with a 2σ external error of better than ±1% on the same diluted NIST U960 standard [34,35].

For Li-isotope analysis, between 50 ml and 400 ml of filtered water were evaporated and passed through cation exchange columns to separate Li [16,36]. Measurements were performed by multi-collector ICP-MS, using a sample-standard bracketing technique, relative to the L-SVEC standard [37], with a concentration within ±10% of that of the sample [16]. Results are presented as δ^7Li, in per mill variations from L-SVEC (where $\delta^7Li = \{[(^7Li/^6Li)_{sample}/(^7Li/^6Li)_{standard}] - 1\} \times 1000$). The 2σ external error based on repeat measurements ($n = 44$) of IAPSO seawater is ±0.90‰.

4. Results

4.1. Physical measurements

Sample locations and field measurements, including pH, temperature, alkalinity, TDS (total dissolved solids) and TSS (total suspended solids) are summarised in Table 1. River waters in the western catchment display a temperature range between 1.5 and 14.9 °C and a pH range between 6.46 and 9.54, while the southeastern rivers show a temperature range between 1.4 and 6.5 °C, and a pH range between 7.72 and 9.69. The observed range of pH is thought to result largely from two counteracting processes: (1) consumption of protons (driving pH to high values) from Fe–Mg silicate dissolution which releases cations into the water; (2) the generation of protons (driving pH to low values) by uptake of CO_2 from the atmosphere via precipitation (e.g. rainfall) and decaying organic matter. Thus, the effect of silicate dissolution on waters originating from the surface of Langjökull icecap can be seen where the pH rises from 6.05 in the meltwater to 6.46 at 300 m from the ice edge, to 7.79 around 4 km from the icecap. In contrast, high pH values are typically seen in groundwaters or those of sub-glacial origin, because such waters have been isolated from atmospheric CO_2. Thus, the Skaftafellsá river dominated by water of sub-glacial origin has a pH of

Table 1
Sample localities and field measurements

Locality	Name	Latitude	Longitude	TDS (mg/l)	TSS (mg/l)	Temp. (°C)	pH	Alkalinity (meq/l)
A1	Exit of Skorradalsvatn	N 64°32.477′	W 21°37.366′	33.8	359	14.9	7.76	0.222
A2	Grímsá river	N 64°32.407′	W 21°20.151′	32.3	569	13.5	8.08	0.405
A3	Grímsá river	N 64°35.576′	W 21°34.753′	40.4	522	12.4	8.07	0.542
A4	Hvítá river at Ferjukot	N 64°36.199′	W 21°42.481′	34.7	612	9.0	7.93	0.473
A6	Norðurá river (Strekkur)	N 64°42.753′	W 21°36.361′	33.9	525	8.8	8.02	0.429
A7	Þverá river	N 64°41.026′	W 21°31.475′	44.8	558	10.0	8.00	0.634
A8	Hvítá river at Kláfoss	N 64°41.612′	W 21°24.867′	26	635	5.6	8.56	0.374
A9	Tributary to Hvítá	N 64°38.925′	W 21°24.740′	58	679	13.8	8.11	0.778
A10	Tributary to Hvítá — water from Ok	N 64°40.813′	W 21°02.309′	20.8	427	11.6	7.83	0.428
A11	Upper Norðurá river	N 64°45.940′	W 21°30.814′	33.1	–	12.5	7.95	0.367
A12	Hvítá river	N 64°42.359′	W 21°02.353′	25.9	–	6.4	9.3	0.469
A13	Norðlingafljót river	N 64°48.101′	W 20°41.306′	60.5	–	12.9	8.44	0.425
A14	Upper Hvítá river	N 64°39.314′	W 20°42.066′	12.03	–	10.1	7.79	0.204
A15	Hvítá river at Langjökull	N 64°38.791′	W 20°34.003′	0.73	–	1.5	6.46	0.0224
A16	Top of Grimsá river	N 64°28.733′	W 20°56.284′	23.1	–	6.6	9.54	0.254
Ice	Meltwater on Langjökull	–	–	0.59	–	0.7	6.05	0.0188
G1	Hraunfossar groundwater	–	–	22.9	–	4.0	9.89	0.249
G2	Hvítá river below Hraunfossar	N 64°42.234′	W 20°59.571′	57.5	–	8.5	9.13	0.342
G3	Hvítá river above Hraunfossar	N 64°42.910′	W 20°50.031′	16.1	–	10.3	8.07	0.217
E1	Skeiðará river	N 63°58.585′	W 16°59.929′	22.1	1890	1.9	9.11	0.324
E2	Jökulsárlón	N 64°02.863′	W 16°10.909′	1479	203	2.1	9.23	0.221
E3	Fjallsárlón	N 64°00.828′	W 16°22.567′	24.8	1380	3.1	9.63	0.332
E4	Virkisá river	N 63°57.280′	W 16°51.100′	6.85	1650	1.4	7.72	0.13
E5	Skaftafellsá river	N 64°00.459′	W 16°56.006′	18.4	2790	1.9	9.69	0.257
E6	Sandgígjukvísl river	N 63°56.707′	W 17°21.020′	15.2	1570	5.5	7.98	0.215
E7	Skaftá river	N 63°46.060′	W 18°07.725′	61.6	845	6.5	8.29	0.933
B4	Hydrothermal spring: Deildartunguhver	N 64°39.864′	W 21°24.740′	1600	–	>100	8.98	–

9.69 and the groundwaters at Hraunfossar a pH of 9.89. The average pH for the western catchment is ~8; for the southeastern rivers the average is 8.8, largely reflecting the effect of glacial cover on water pH.

Alkalinity (which is mainly contributed by HCO_3^-), determined by in situ titration, ranges from 0.019 mmol/l in meltwater directly on the glacier to 0.933 mmol/l in the longer rivers. Again, in water flowing off Langjökull, alkalinity increases from 0.019 to 0.022 in 300 m and to 0.20 within a 4 km distance. As one of the driving forces which controls pH, higher alkalinity generally indicates more contact with atmospheric CO_2.

The average water temperature in the western catchment is ~10 °C, whereas for the southeastern catchment the average temperature is 3.2 °C, with colder water associated with glacial runoff.

In the western catchment TDS range from 0.59 mg/l in the meltwater to 58 mg/l in the Hvítá River close to hot spring input (at Deildartunguhver) which itself has a TDS of 1600 mg/l. As with pH, in general, TDS increases rapidly away from the edge of Langjökull icecap. Excluding hydrothermal input, the average TDS for the western catchment is 25.2 mg/l, close to average values for Iceland [5,38]. The southeastern rivers display highly variable TDS ranging from 15.2 to 1479 mg/l (for Jökulsárlón, which is connected to seawater). For the western catchment low TDS is associated with low pH, corresponding to the glacial surface waters. However, regional studies have shown that TDS also decreases with increasing age of the basalt in the watershed. This has been taken to suggest that younger basalts are more susceptible to weathering relative to older basalts. Thus, the high TDS of some of the southeastern rivers may be attributed, at least in part, to the younger age of the basalts, but perhaps also in part to the presence glass-rich basalt (hyaloclastite) under the icesheet, where glass is even more susceptible to weathering than crystalline basalt [5,17,39].

4.2. Major and trace elements

Major cation concentrations from the bedload and suspended load are given in Table 2. Bedload Ca/Na and Mg/Na ratios vary between 7.04 and 14.5 and between 3.11 and 10.4 respectively. Rocks taken from the western catchment by Gíslason et al. [5] have Ca/Na and Mg/Na values of 3.2–5.6 and 1.2–3.8 respectively. The difference in values can be explained by the greater mobility

Table 2
Concentrations of major elements and uranium and lithium isotope ratios for the bedloads (Bed) and suspended loads (Susp) of Iceland rivers

		Na (mg/g)	Al (mg/g)	Si (mg/g)	K (mg/g)	Ca (mg/g)	Li (μg/g)	Mg (mg/g)	Th (μg/g)	^{238}U (μg/g)	δ^7Li (‰)	(^{234}U/^{238}U)†
A1	Bed	6.86	25	225	1.61	69.8	7.44	34.2	2.04	0.521	5.6	0.961±11
A2	Bed	5.7	26.4	217	0.85	77.7	7.34	45.9	0.929	0.242	5.8	1.10±2
	Susp						2.2*			0.0488	6.0	1.24±1
A3	Bed	5.77	27.7	218	0.925	77.2	7.6	39.7	0.945	0.482	5.2	1.10±1
	Susp						3.0*			0.261	5.0	1.00±1
A4	Bed	5.66	25.1	227	0.658	82.1	4.57	58.8	0.548	0.136	2.8	1.04±1
	Susp	5.77	32.1	–	0.828	76.6	5.49	33	0.699	0.196	0.9	1.04±2
A6	Bed	7.48	27.2	248	2.98	52.7	11.0	23.3	2.88	0.727	8.9	0.999±20
	Susp						4.4*			0.0499	0.4	1.26±2
A7	Bed	7.25	25.2	223	1.35	73.7	7.56	33.8	1.77	0.42	6.5	0.998±7
	Susp									0.0521	2.8	1.47±2
A8	Bed	5.82	25.9	232	1.23	77.9	6.33	56	1.17	0.329	5.1	1.03±1
	Susp	5.69	31.1	–	0.69	77.8	5.67	35.9	0.65	0.172	4.4	1.04±1
A9	Bed	7.82	25.1	241	2.75	62.5	8.12	29.6	2.95	0.701	4.7	0.990±21
	Susp						7.0*			0.0944	−0.6	1.04±1
A10	Bed	6.55	26.3	229	1.69	72.1	6.43	39.1	1.41	0.398	5.8	1.00±1
	Susp									0.0598	4.4	1.32±1
E1	Bed	7.4	25	231	1.47	76.4	6.58	37.6	1.15	0.331	3.5	1.04±2
	Susp	5.33	28.6	–	2.5	64.4	14.3	39.9	3.08	0.782	1.4	0.989±8
E2	Susp	8.03	29.1	–	4.02	55.4	13.1	37.2	2.44	0.69	2.9	1.04±1
E3	Susp	4.23	19.5	–	3.35	29.8	15.1	25.8	2.52	0.754	0.6	1.05±1
E4	Susp	4.54	15.0	–	2.78	23.1	11.2	10.7	3.49	0.797	3.2	1.02±1
E5	Bed	8.65	25.5	234	2.68	66.7	7.45	29	2.25	0.634	4.7	1.01±1
	Susp	4.74	22.6	–	2.62	43.8	14.5	33.1	3.41	0.885	3.9	1.00±1
E6	Susp	3.6	14.1	–	0.869	35.2	4.74	17.3	0.816	0.212	7.5	1.05±2
E7	Bed	7.3	24.5	232	1.49	70	7.26	33.5	1.17	0.337	4.6	
	Susp	1.11	11.4	–	0.472	20.1	3.87	19.1	1.19	0.279	−1.3	1.00±2

*Concentrations calculated from MC-ICP-MS voltages relative to voltage of standard of known concentration (error±10%).
†Internal error (2σ) is reported for (^{234}U/^{238}U).

of Na in aqueous environments compared to Ca and Mg [5], indicating at least some chemical weathering of the bedload.

Suspended load Ca/Na ratios vary from 5.1 to 18.1; Mg/Na ratios from 2.4 to 17.2. This greater range of values than shown in the bedload indicates a greater variety in the degree of chemical weathering the suspended load has been subjected to.

U/Th ratios are similar in the river sands (average of 0.29) and suspended material (0.28). The mean U/Th ratio for fresh Icelandic basalts is 0.31 [40,41], indicating that both sands and suspended material are not significantly depleted in these elements relative both to each other and to unweathered source rock [38]. This suggests that U is significantly less mobile than Na and that the residence time for suspended particles in these rivers is relatively short.

The concentrations for the same elements and major anions are shown for the dissolved load in Table 3. Where appropriate these concentrations have been corrected for rainwater input, by assuming that all chloride content of the river waters (Table 3) is of atmospheric origin and using the X/Cl ratio of the sampled ice as representing meteoric water [4]. This hypothesis is validated by the low chloride concentrations of Icelandic basaltic rocks [5]. The magnitude of this correction was up to ~70%. A similar approach was made to correct the river waters for hydrothermal spring inputs. Directly sampled hydrothermal springs are over 100× enriched in SO_4^{2-} relative to river waters (Table 3), so SO_4^{2-} can be used to correct elemental concentrations [42].

For all river waters, the molar Ca/Na ratio is between 0.01 and 2.4, with slightly higher values in the southeastern catchment, due to lower Na concentrations there.

The mass ratio of U/Th in the riverine dissolved load ranges from 0.13 to 2530, with an average value of 160. This illustrates the preferential release of U relative to Th into waters, due to the greater mobility of U relative to Th during chemical weathering. Low river values may be due to hydrothermal input (U/Th=0.47) or groundwater input (U/Th=0.96). Both of these ratios are closer to the rock values, probably due to more congruent chemical weathering of both elements in hydrothermal and groundwater environments.

Table 3
Elemental and isotopic compositions of the dissolved load of rivers, ice and hydrothermal springs, in Iceland

	Na (μmol/l)	Mg (μmol/l)	Al (μmol/l)	Si (μmol/l)	K (μmol/l)	Ca (μmol/l)	Cl^- (μmol/l)	NO_3^- (μmol/l)	SO_4^{2-} (μmol/l)	Li (nmol/l)	Th (pmol/l)	^{238}U (pmol/l)	δ^7Li (‰)	$(^{234}U/^{238}U)^{\dagger}$
A1	303	64.2	0.183	114	6.85	68.2	379	20.6	5.02	2.12	0.166	98.4	43.7	1.67±1
A2	324	64.6	0.313	170	9.84	86.8	282			21.9		36.5	25.4	1.51±2
A3	361	98.4	0.253	226	11.0	112	402	25.4	3.03	15.6	0.191	63.0	34.5	1.88±1
A4	309	76.2	1.19	219	12.1	98.1	361		4.75	41.8	0.401	16.1	21.1	1.57±2
A6	283	73.8	0.188	168	8.61	109	312	34.9	5.49	5.66	0.726	15.0	36.8	1.72±2
A7	362	126	0.162	198	17.3	129	434	70.2		41.0	0.362	28.2	26.2	1.73±1
A8	270	43.1	2.14	205	10	74.3	236	54.6	8.33	31.9	0.567	10.7	21.5	1.50±2
A9	509	150	0.365	285	17.5	150	414	22.9	27.7	43.5		16.7	18.7	1.44±2
A10	282	60.5	0.622	225	9.77	85.6	325	15.3		4.95	0.166	4.45	33.6	2.41±1
A11	306	74.7	0.117	226	9.55	120	140	29.0	15.2	7.76	18.9	4.03	28.2	1.71±1
A12	267	34	2.69	235	8.96	69.8	62.3	9.21	11.2	37.5	7.16	19.0	18.5	1.39±2
A13	311	66.8	0.909	242	19.4	91.6	83.8	8.45	7.85	75.6	4.68	40.7	23.7	1.86±2
A14	125	43.9	0.757	134	5.32	57.3	28.0	12.8	9.42	141	1.86	15.2		1.28±2
A15	4.82	1.39	0.124	5.71	0.63	7.25	3.06	4.24		1.54	6.10	0.753		1.70±3
A16	255	33	1.25	278	11.7	68.0	100	3.68	10.2	26.3	6.14	11.7		1.29±2
G1	280	27.1	1.84	278	9.90	62.4	59.6	3.54	10.8	35.1	14.5	13.6	22.9	1.37±1
G2	367	40.3	1.73	302	10.8	78.6	76.4	8.36	13.8	52.7	9.58	17.7	20.2	1.57±2
G3	187	22.1	1.31	177	6.13	57.2	40.6	9.20	7.31	39.2	5.82	7.37		1.76±2
E1	205	27.2	3.54	70.4	4.89	106	163		41.2	55.9	9.20	34.0	21.0	1.70±4
E2	20900	2360		113	540	653	55500		606	1250		550	34.1	1.19±1
E3	65.8	16.6	4.97	30.4	3.64	160	164	21.0	52.3	9.20		30.2	26.5	2.17±2
E4	117	15.2	0.216	59.6	13.3	27.9	166	19.5		60.8	0.106	2.87	18.5	1.49±2
E5	132	13.2	3.612	45.7	3.64	92.1	180	70.8		16.3	3.25	54.1	23.1	1.60±1
E6	136	19.9	0.793	74.9	4.28	60.9	112	69.7	30.8	24.0	0.182	3.46	17.0	1.31±1
E7	341	110	0.578	282	12.8	347	165	8.00	135	145	0.0330	80.6	16.3	1.13±1
Ice	61.1	6.7	0.046	3.3	1.01	0.700	6.82	72.7		2.12		1.14	33.3	
B4	23600	2410		2120	614	584	21600		1540	5170	150	69.4	10.9	0.860±19

These data have not been corrected for hydrothermal and rainwater input.
†Internal error (2σ) is reported for $(^{234}U/^{238}U)$.

4.3. Uranium elemental and isotope data

The concentrations and activity ratios of uranium are given in Table 2 for the bedloads and suspended loads. ^{238}U concentration in the bedload varies between 0.05 and 0.73 ppm and between 0.05 and 0.89 ppm in the suspended load. These concentrations lie in the same range as basalts from the Snæfellsnes lava field to the north [43]. $(^{234}U/^{238}U)$ activity ratios in the bedload range from 0.96 to 1.09, where an activity ratio of 1 is secular equilibrium. In the suspended load, the activity ratio ranges from 1.00 to 1.32. There is no relationship between $(^{234}U/^{238}U)$ values of the bedloads and suspended loads.

^{238}U concentrations in the dissolved load of the rivers range from 0.75 to 98 pmol/l and are given in Table 3. Low concentrations are seen close to the icecaps, in which the ice itself has a ^{238}U concentration of 1.14 pmol/l, and then increase as the water progresses through the river catchment (Fig. 2). Hydrothermal springs have a ^{238}U concentration of almost 70 pmol/l and an activity ratio of 0.86. Hydrothermal corrections have been performed on samples with known hydrothermal input (samples A8 and A9). Corrections were made by assuming two-component mixing between the hydrothermal and precipitation-corrected river water end-members. Corrections altered the activity ratio by approximately 20%. $(^{234}U/^{238}U)$ in the dissolved load ranges from 1.13 to 2.41. High activity ratios are associated with rivers directly fed by glaciers. Therefore, waters with low U concentrations and high activity ratios are seen close to the source of glacial rivers. Non-glacial rivers initially have low U concentrations and low activity ratios, both of which increase as the water progresses through the river system. This effect cannot be due to hydrothermal input, as this has high concentrations and low activity ratios. There is a slight positive trend between the activity ratios of the suspended load and dissolved load, with higher $(^{234}U/^{238}U)$ in the suspended load correlating with higher values in the dissolved load.

4.4. Lithium elemental and isotope data

Li concentrations and Li isotope values are given for the bedload and suspended load in Table 2. The Li

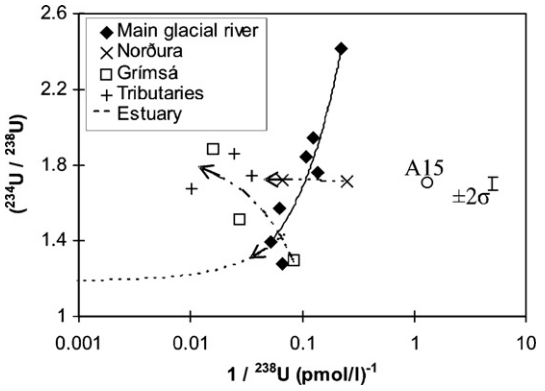

Fig. 2. Relationship between U activity ratio (^{234}U /^{238}U) and ^{238}U concentration (reported as 1/^{238}U) for the dissolved load in the western catchment. Arrows show movement of water downstream in the main glacial river (Hvita; solid black line) and the non-glacial rivers (Norðura, dashed grey line and Grímsá, dashed black line). Dotted black line shows how river water values progress into estuary values [49]. Error bar shows the external error on (^{234}U/^{238}U) (2σ); the external error on ^{238}U concentration is smaller than the symbols.

concentration varies from 4.57 to 11.0 ppm in the bedload and from 2.1 to 15.1 ppm in the suspended load. Whole rock basalt samples (e.g. from the Laki basalt) show concentrations within this range [15]. The δ^7Li isotope composition in the bedload and suspended load varies from 2.8 to 8.9‰ and from −1.3 to 7.5‰ respectively.

The Li concentrations and isotope ratios for the dissolved load are given in Table 3. In the riverine dissolved load the Li concentration ranges from 1.54 nmol/l close to glaciers to 145 nmol/l in rivers which may have hydrothermal influence. Ice itself has a concentration of 2.12 nmol/l; hydrothermal waters have a Li concentration of over 5000 nmol/l. The δ^7Li values

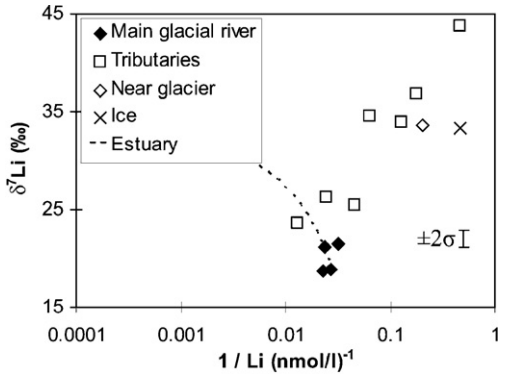

Fig. 3. Relationship between δ^7Li and Li concentration of the dissolved load of western rivers. Dotted black line shows how river water values progress into estuary values [49]. Error bar shows the external error on δ^7Li (2σ); the external error on the Li concentration is smaller than the symbols.

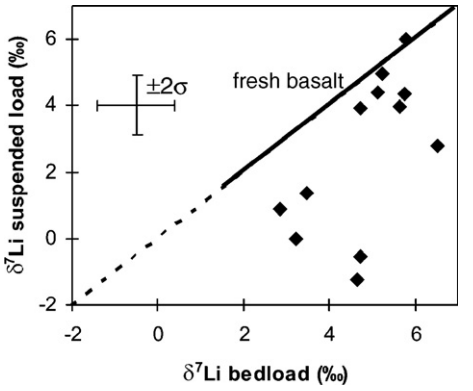

Fig. 4. δ^7Li values of the suspended and bed sediments in Icelandic rivers. The dashed line represents equal values; the solid region shows the range for fresh basalt reported by [50,51].Error bars show the external error (2σ).

in the dissolved load range from 17.0 to 43.7‰ (Fig. 3). The Li isotope ratio measured in ice taken from Langjökull is identical to that of seawater, suggesting that for Li, precipitation over this part of Iceland is dominated by input of oceanic aerosols. δ^7Li in hot spring waters is 10.9‰. Hydrothermal corrections were performed in a similar manner to those for uranium isotope ratios (Section 4.3) using the measured value for the hydrothermal input. The corrections comprise an adjustment of 14 to 30% of the δ^7Li values.

The δ^7Li value of the suspended load is always lower than that of the corresponding bedload, due to the preferential mobilisation of the heavy Li isotope during weathering (Fig. 4). High δ^7Li in the dissolved load is associated with glacial and immature rivers and potentially groundwater input (22.8‰ at Hraunfossar).

5. Discussion

5.1. Physical and chemical erosion rates

Physical or mechanical erosion rates reflect the amount of sediment removed from the catchment area by rivers. Averaged hourly discharge rates given for 2003 by the Iceland National Energy Authority (pers. comm.) compare well with those given by Gíslason et al. [5], and combined with TSS data obtained here (Table 1), give an estimate of the instantaneous physical erosion rate. These range between 920 and 1160 t/km^2/yr, with an average of 1075 t/km^2/yr, for the western field area, with higher rates associated with glacier-fed rivers. This is higher than the mean physical erosion rate for Iceland of 500 t/km^2/yr [5], which does not include glacial outburst floods, but within the range of 21 to 4864 t/km^2/yr given by [38] for the whole island. Differences

in measured TSS and discharge due to seasonal variations may account for the variations in erosion rates. Except for the Skaftá River, the lack of discharge rate measurements on the unstable rivers south of Vatnajökull make erosion rate estimates impossible. Data from this study give the Skaftá an instantaneous mechanical weathering rate of 2084 t/km^2/yr.

Chemical erosion rates represent the flux of dissolved solids in rivers and can be estimated using TDS data (Table 1). Estimated instantaneous chemical erosion rates vary from 45 to 91 t/km^2/yr, generally with lower rates associated with glacier-fed rivers. The highest value (sample A9) does stem from a glacier-fed river. However this sample is also associated with hydrothermal input, which has a high TDS (Table 1). A hydrothermal correction can be performed as detailed in Section 4.2, which gives a revised chemical erosion rate of 36 t/km^2/yr. These values compare well with those given by [5,20,38] (on average 55 t/km^2/yr for SW Iceland and 37 t/km^2/yr for the whole of Iceland). The Skaftá River in the south of Iceland has chemical weathering rates of 150 t/km^2/yr.

5.2. Mineral saturation states

Primary mineral dissolution due to weathering and secondary mineral formation constitutes the most important process which influences surface water chemistry [27,44]. The stability of primary basaltic minerals under Icelandic weathering conditions is not only controlled by dissolution rate, but also by the formation of secondary minerals and biomass. Major element consumption by secondary mineral formation and biomass maintains primary mineral undersaturation in rivers, which, as a result, continue to dissolve. Both primary and secondary mineral saturation states have been calculated using the program PHREEQC for Windows [45], which estimates mineral stability from the degree of over- or understauration in terms of Gibbs free energy (kJ). This is denoted by the saturation index (SI). SI values >1 show oversaturation, whereas values <1 show undersaturation. In situ pH and temperature, measured anion and cation concentrations, as well as calculated pE values were used for these calculations. The overall uncertainties on calculated saturation indices are likely to be within 1–2 SI units (cf. [26]).

Primary minerals such as olivine, clinopyroxene and plagioclase are undersaturated in the ice-melt, river waters and in most groundwaters (Fig. 5). The degree of undersaturation for all these minerals decreases with increasing pH and clinopyroxene shows values approaching saturation in the groundwaters at high pH, consistent with previous data for Icelandic rivers [26,27]. The high weathering susceptibility of olivine is shown by its high degree of undersaturation.

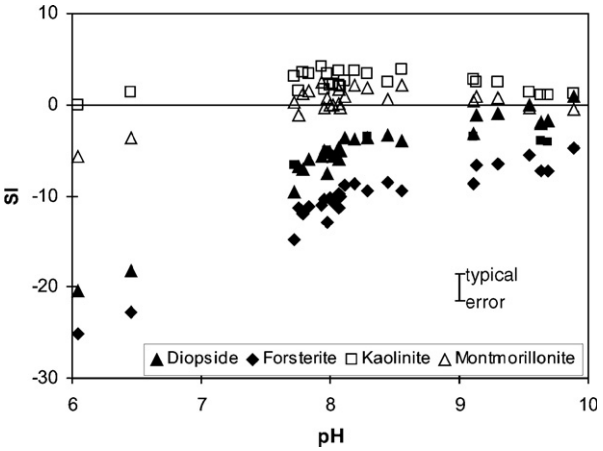

Fig. 5. Saturation index (SI; see text for details) of primary (closed symbols) and secondary (open symbols) minerals in Icelandic rivers as a function of their in situ pH. SI values of >0 indicate oversaturation; values of <0 indicate undersaturation.

Secondary minerals, such as clay minerals and the primary mineral magnetite, in general show oversaturation, indicating potential formation and precipitation of these secondary minerals, and the stability of magnetite, in the rivers sampled. At low pH values of 6–6.5, these minerals tend to be saturated or slightly undersaturated, and reach roughly constant degrees of oversaturation by pH 8 (Fig. 5).

5.3. Uranium isotope ratios

U activity ratios from the bedload for both the western and southeastern rivers show that the system is mature enough to have reached secular equilibrium ((^{234}U/^{238}U)=1). Suspended load samples with values higher than 1 have probably adsorbed U from the dissolved load, which may explain the positive correlation between activity ratios in the suspended and dissolved loads. There are no suspended sediments characterised by activity ratios lower than 1, indicating that preferential leaching of the suspended sediments by the dissolved load is not occurring to any resolvable degree. Instead, dissolved load data show that the primary source of the ^{234}U excess is not in-river sediment leaching, but α-recoil effects associated with glacial weathering products at river sources.

This is shown by the high (^{234}U/^{238}U) values in the dissolved load close to the glacier. Fig. 2 shows a mixing diagram of (^{234}U/^{238}U) against 1/^{238}U for the western catchment. As uranium concentrations increase almost

linearly with distance through the river system (similar behaviour has been seen in a Baltic Shield watershed [9] and in the Strengbach watershed [46]), this diagram essentially shows position in the catchment relative to ice edge. The main glacier-fed (Hvítá) river shows high activity ratios and low concentrations close to the glaciers. Note that the sample with the highest ($^{234}U/^{238}U$) value (A10) does not actually come from the Hvítá, but is a tributary fed by the Ok glacier rather than the Langjökull icecap. These high ($^{234}U/^{238}U$) values are then progressively diluted by tributaries, which have lower activity ratios, entering the river. Additional dilution occurs by congruent chemical weathering in the Hvítá River itself and by groundwater input with low ($^{234}U/^{238}U$) (the groundwater sample taken, G1, has an activity ratio of 1.37). The only deviation from this dilution gradient is shown by sample A15 (Fig. 2), which was taken 300 m from the glacier edge. This may be due to the fact that this water is essentially meltwater running off the top of the glacier (which is likely to have oceanic activity ratios), which has not yet been exposed to significant water-rock interaction.

The tributaries flowing into the main river tend to be characterised by lower activity ratios and higher concentrations than most of the glacial rivers. The higher concentrations are probably due to the fact that these rivers (unlike glacial rivers) are not being significantly diluted by glacial meltwater with extremely low concentrations. The input of these waters into the river system progressively reduces the activity ratio of the dissolved load downstream. This suggests that in glacial rivers the most extreme uranium isotope fractionation occurs close to the glacier itself. This is due to the increase in the ratio of surface area to volume of the sediment clasts, caused by glacial weathering which, in turn, results in an increase in the amount of ^{234}U from α-recoil in the dissolved load. This is in contrast to the non-glacial tributaries sampled in this study (Fig. 2) and the Strengbach river sampled by Riotte and Chabaux [46], which show an increase of uranium activity ratios downstream (the Grímsá River, whereas the other non-glacial Norðura River shows unchanging activity ratios).

In effect, as the ^{234}U enrichment in the dissolved load is due to α-recoil from fine-grained material formed by mechanical weathering, the dissolved load ($^{234}U/^{238}U$) is acting as a tracer of physical weathering. This then demonstrates the difference in the degree of physical weathering between glacial and non-glacial rivers: in glacial rivers, the dominant grain comminution is at or close to the glacier, whereas in non-glacial rivers primary physical weathering occurs in the river system itself.

5.4. Li-isotopes

Most studies of Li-isotope behaviour in continental weathering environments suggest that δ^7Li values do not directly reflect the catchment lithology, but instead are controlled by fractionation during the weathering process [12–15]. The δ^7Li values measured in river waters here are on average 20‰ higher than those measured in the suspended load. Experimental work shows no evidence for significant variation during partial dissolution of basalts, implying a uniformity in Li-isotope ratios between basaltic minerals [15], so the difference between the δ^7Li values of the dissolved and suspended loads must be due to retention of ^6Li in secondary mineral phases during the weathering process.

The effects of secondary mineral formation on the δ^7Li value of the dissolved load are explored further in Fig. 6. This figure shows that as the saturation index of secondary minerals (represented here by kaolinite, the most stable Al/Si clay mineral formed in Icelandic soils, and montmorillonite) increases, the δ^7Li value of the dissolved load decreases. This correlation is significant at the 95% confidence level. This suggests that as the water becomes increasingly saturated, secondary mineral precipitation speeds up and so isotope fractionation between Li in the secondary minerals and Li in solution is reduced and relatively more ^6Li remains in solution.

Fig. 6, together with other studies [11,14], implies that Li-isotope variations in rivers may reflect the intensity of silicate weathering. Fig. 7 shows δ^7Li for the dissolved load plotted against dissolved silicon concentrations for both Icelandic river systems. In most river systems, Si is not straight forward tracer of silicate weathering, because Si rapidly enters the biogeochemical cycle and is removed from aqueous systems [47].

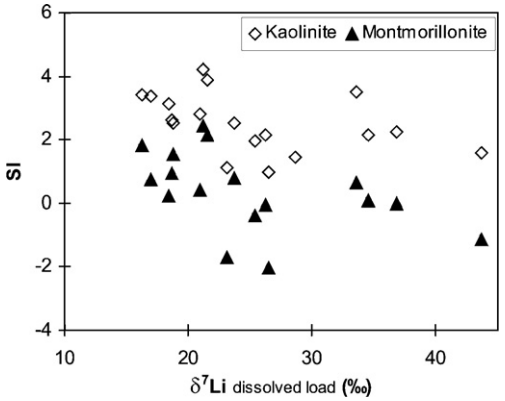

Fig. 6. Saturation index (SI; see text for details) of secondary minerals (kaolinite and montmorillonite) relative to δ^7Li of the dissolved load of Icelandic rivers.

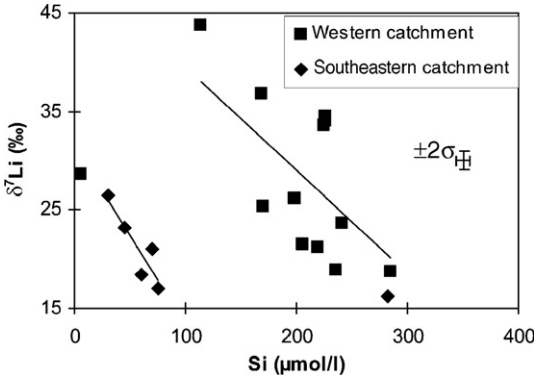

Fig. 7. Relationship between δ^7Li and Si concentration for the dissolved load of Icelandic rivers. Error bars show the external error (2σ).

However, in the barren glacial areas of Iceland, biological activity is limited, and dissolved Si concentrations are more likely to reflect silicate weathering. Both catchments show a negative trend, with low δ^7Li corresponding to high Si concentrations, and vice versa. This suggests that with greater weathering intensity (high Si), the degree of Li isotope fractionation between the suspended and dissolved load decreases (cf. Huh et al. [12]). Each catchment exhibits a distinct trend, with the southeastern rivers having a much lower Si concentration for a given δ^7Li value. It is interesting to note that the one long river sampled in the southeast (the Skaftá River which is almost 80 km long from source to sampling point) shows a similar relationship to the more mature western rivers. Also, the ice sample, with a low Si concentration, plots on an extension of the trend defined by the southeastern rivers. This suggests that the different trends are the result of differences in the river source. In the southeast, the source is the icecap, with low Si concentrations and δ^7Li=33.3‰. The western catchment has sources other than glacial inputs, with higher Si and δ^7Li.

An analysis of the mixing of Li and its isotopes in the western catchment, similar to that performed for U-isotopes in Fig. 2, shows a more complex signal than that for uranium. Fig. 3 shows that, with the exception of the samples taken from close to the glacier, the main glacial (Hvítá) river has relatively low δ^7Li values (18.7–21.5‰). However, its tributaries, as well as the ice and near-glacier samples, appear to show a trend of high δ^7Li values corresponding to low Li concentrations. This suggests that the main control on the Li-isotope composition of the glacial-fed river cannot be precipitation flowing off Langjökull icecap or inputs from its tributaries, as the δ^7Li values of these sources are too high. Rather, superficial chemical weathering creates a high δ^7Li in waters close to the glacier and from short tributaries, while continued weathering of suspended material in the main, more mature, river system increases the saturation state of the dissolved load with respect to secondary minerals, leading to lower δ^7Li values for its dissolved load. Thus, overall these data suggest that lithium isotope variations generally reflect the degree of chemical weathering intensity in Icelandic rivers.

5.5. Glacial rivers

If uranium isotopes essentially reflect physical or glacial weathering and lithium isotopes reflect the chemical weathering intensity, then the combination of the two systems should, in theory, give information on the balance of physical and chemical weathering. Fig. 8 shows the uranium activity ratios against the lithium isotope ratio for the southeastern rivers which flow out of the Vatnajökull icecap and also for the dominantly glacial rivers from the western catchment. These data illustrate a positive correlation between the two isotope systems for glacial rivers, which is not observed for non-glacial rivers.

The increase in uranium activity ratios corresponds to an increase in physical (glacial) weathering. This is due to the presence of fine-grained till produced by glacial grinding resulting in a greater ratio of surface area to volume of sediment clasts for α-recoil effects, which enriches the dissolved load in ^{234}U [48]. In contrast, the corresponding increase in δ^7Li is due to a reduction in chemical weathering intensity; if chemical weathering is low, ^{6}Li is preferentially retained in secondary minerals. Thus, if physical comminution of grains by glaciers is high, the corresponding chemical weathering intensity is

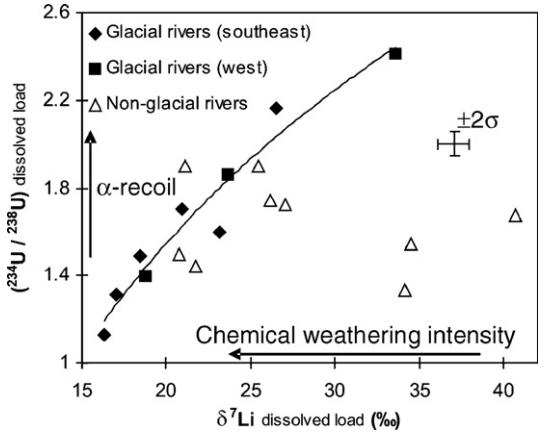

Fig. 8. U activity ratio (^{234}U / ^{238}U) versus δ^7Li of the dissolved load of Icelandic rivers. Error bars show the external error (2σ).

low, and vice versa. This is consistent with the observation that glacial cover locally reduces chemical weathering [5], by inhibiting contact with atmospheric CO_2 and thereby raising water pH, and stabilising primary Ca and Mg silicates.

6. Conclusions

The major conclusions from this study are as follows:

1. Uranium activity ratios indicate that the Hvítá River, which runs off the Langjökull icecap in the west of Iceland, exhibits simple dilution of glacial water, which has a large dissolved component from mechanical weathering with low uranium concentration and high ($^{234}U/^{238}U$), by rivers with a greater degree of more congruent weathering and with high uranium concentrations and low ($^{234}U/^{238}U$) and groundwater with low uranium concentrations and activity ratios. The reason for high activity ratios in the glacial water is likely due to increased surface area in glacial sediment enriching the water in ^{234}U due to α-recoil. The decrease in activity ratios is in contrast to non-glacial rivers from both this and other studies [9,46], where activity ratios increase through the river system. Thus, in this basaltic terrain, at least, uranium activity ratios appear to reflect the degree of physical weathering by glaciers.
2. δ^7Li values for the dissolved load are always greater than those of the corresponding suspended load because ^{6}Li is preferentially retained in secondary minerals. Lithium isotope ratios for the dissolved load decrease with increasing silicon concentrations, suggesting that δ^7Li is related to the degree of weathering of silicate material. River water which is oversaturated with secondary minerals has lower δ^7Li because secondary mineral precipitation will be rapid and so isotope fractionation between Li in the secondary minerals and Li in solution is reduced.
3. The behaviour of Li-isotopes in the western Hvítá catchment is somewhat more complicated than that of uranium isotopes. Mature rivers which are saturated with respect to secondary minerals have relatively low δ^7Li values. However, a second component is introduced in the upper areas of the river close to the glacier, with a much higher δ^7Li. This, and the fact that the tributaries have higher δ^7Li than most of the main river, indicates that the behaviour of Li-isotopes in river systems is not simply a function of initial input and then dilution, but of isotope ratios changing in the river itself due to changes in the weathering regime.
4. Rivers sourced directly from glaciers, such as those in the southeast of Iceland and those close to the icecap in the west of Iceland show a co-variation between lithium and uranium isotopes, despite Li fractionation being due to mass-dependence and U due to α-recoil. This behaviour suggests that for glacier-fed rivers chemical weathering intensity is inversely related to physical weathering rate.

Acknowledgements

We would like to thank Abdelmouhcine Gannoun, Nick Rodgers, Mabs Gilmour, Louise Thomas, Jason Harvey, Josh Wimpenny, Natalie Vigier, John Watson and Anthony Cohen for their help and advice in the completion of this project. This manuscript was greatly improved by the constructive comments of Jerome Gaillardet, Paul Tomascak, and two anonymous reviewers.

References

[1] C. Dessert, B. Dupre, J. Gaillardet, L.M. Francois, C.J. Allegre, Basalt weathering laws and the impact of basalt weathering on the global carbon cycle, Chem. Geol. 202 (3–4) (2003) 257–273.
[2] J. Gaillardet, B. Dupre, P. Louvat, C.J. Allegre, Global silicate weathering and CO_2 consumption rates deduced from the chemistry of large rivers, Chem. Geol. 159 (1–4) (1999) 3–30.
[3] J.C.G. Walker, P.B. Hays, J.F. Kasting, A negative feedback mechanism for the long-term stabilization of earths surface-temperature, J. Geophys. Res. -Oceans Atmos. 86 (NC10) (1981) 9776–9782.
[4] P. Louvat, C.J. Allegre, Riverine erosion rates on Sao Miguel volcanic island, Azores archipelago, Chem. Geol. 148 (3–4) (1998) 177–200.
[5] S.R. Gislason, S. Arnorsson, H. Armannsson, Chemical weathering of basalt in southwest Iceland: effects of runoff, age of rocks and vegetative/glacial cover, Am. J. Sci. 296 (8) (1996) 837–907.
[6] M. Frank, Radiogenic isotopes: tracers of past ocean circulation and erosional input, Rev. Geophys. 40 (1) (2002) art. no.-1001.
[7] P.W. Swarzenski, D. Porcelli, P.S. Andersson, J.M. Smoak, The behavior of U- and Th-series nuclides in the estuarine environment, Uranium-Series Geochemistry, Reviews in Mineralogy and Geochemistry, vol. 52, 2003, pp. 577–606.
[8] P. Swarzenski, P. Campbell, D. Porcelli, B. McKee, The estuarine chemistry and isotope systematics of U-234,U-238 in the Amazon and Fly Rivers, Cont. Shelf Res. 24 (19) (2004) 2357–2372.
[9] D. Porcelli, P.S. Andersson, M. Baskaran, G.J. Wasserburg, Transport of U- and Th-series nuclides in a Baltic Shield watershed and the Baltic Sea, Geochim. Cosmochim. Acta 65 (15) (2001) 2439–2459.
[10] N. Vigier, K.W. Burton, S.R. Gislason, N.W. Rogers, B.F. Schaefer, R.H. James, Constraints on basalt erosion from Li isotopes and U-series nuclides measured in Iceland rivers, Geochim. Cosmochim. Acta 66 (15A) (2002) A806–A806.
[11] B. Kisakurek, R.H. James, N.B.W. Harris, Li and delta Li-7 in Himalayan rivers: proxies for silicate weathering? Earth Planet. Sci. Lett. 237 (3–4) (2005) 387–401.

[12] Y. Huh, L.H. Chan, L. Zhang, J.M. Edmond, Lithium and its isotopes in major world rivers: implications for weathering and the oceanic budget, Geochim. Cosmochim. Acta 62 (12) (1998) 2039–2051.
[13] Y. Huh, L.H. Chan, J.M. Edmond, Lithium isotopes as a probe of weathering processes: Orinoco River, Earth Planet. Sci. Lett. 194 (1–2) (2001) 189–199.
[14] Y. Huh, L.H. Chan, O.A. Chadwick, Behavior of lithium and its isotopes during weathering of Hawaiian basalt, Geochem. Geophys. Geosyst. 5 (2004) art. no.-Q09002.
[15] J.S. Pistiner, G.M. Henderson, Lithium-isotope fractionation during continental weathering processes, Earth Planet. Sci. Lett. 214 (1–2) (2003) 327–339.
[16] B. Kisakurek, M. Widdowson, R.H. James, Behaviour of Li isotopes during continental weathering: the Bidar laterite profile, India, Chem. Geol. 212 (1–2) (2004) 27–44.
[17] D. Wolff-Boenisch, S.R. Gislason, E.H. Oelkers, The effect of crystallinity on dissolution rates and CO_2 consumption capacity of silicates, Geochim. Cosmochim. Acta 70 (4) (2006) 858–870.
[18] S.R. Gislason, H.P. Eugster, Meteoric water–basalt interactions. 2. A laboratory study, Geochim. Cosmochim. Acta 51 (10) (1987) 2827–2840.
[19] A. Stefansson, S.R. Gislason, Chemical weathering of basalts, Southwest Iceland: effect of rock crystallinity and secondary minerals on chemical fluxes to the ocean, Am. J. Sci. 301 (6) (2001) 513–556.
[20] S.R. Gislason, Chemical weathering, chemical denudation and the CO_2 budget for Iceland, in: C.J. Caseldine, A. Russell, J. Hardardóttir, O. Knudsen (Eds.), Iceland: Modern processes, Past Environments, Elsevier, 2005, pp. 289–307.
[21] O.S. Pokrovsky, J. Schott, Kinetics and mechanism of forsterite dissolution at 25 degrees C and pH from 1 to 12, Geochim. Cosmochim. Acta 64 (19) (2000) 3313–3325.
[22] E.H. Oelkers, An experimental study of forsterite dissolution rates as a function of temperature and aqueous Mg and Si concentrations, Chem. Geol. 175 (3–4) (2001) 485–494.
[23] E.H. Oelkers, J. Schott, An experimental study of enstatite dissolution rates as a function of pH, temperature, and aqueous Mg and Si concentration, and the mechanism of pyroxene/pyroxenoid dissolution, Geochim. Cosmochim. Acta 65 (8) (2001) 1219–1231.
[24] E.H. Oelkers, General kinetic description of multioxide silicate mineral and glass dissolution, Geochim. Cosmochim. Acta 65 (21) (2001) 3703–3719.
[25] S.R. Gislason, E.H. Oelkers, Mechanism, rates, and consequences of basaltic glass dissolution: II. An experimental study of the dissolution rates of basaltic glass as a function of pH and temperature, Geochim. Cosmochim. Acta 67 (20) (2003) 3817–3832.
[26] A. Stefansson, S.R. Gislason, S. Arnorsson, Dissolution of primary minerals in natural waters — II. Mineral saturation state, Chem. Geol. 172 (3–4) (2001) 251–276.
[27] S.N. Arnorsson, I. Gunnarsson, A. Stefansson, A. Andresdottir, A.E. Sveinbjornsdottir, Major element chemistry of surface — and ground waters in basaltic terrain, N-Iceland. I. Primary mineral saturation, Geochim. Cosmochim. Acta 66 (23) (2002) 4015–4046.
[28] S. Moorbath, H. Sigurdss, R. Goodwin, K–Ar ages of oldest exposed rocks in Iceland, Earth Planet. Sci. Lett. 4 (3) (1968) 197.
[29] Norddahl, Petursson, Relative sea level changes in Iceland: new aspects of the Weichselian deglaciation of Iceland, in: C.J. Caseldine, A. Russell, J. Hardardóttir, O. Knudsen (Eds.), Iceland: Modern Processes, Past Environments, Elsevier, 2005, pp. 25–78.
[30] F. Sigurdsson, J. Ingimarsson, The permeability of Icelandic rocks, in: G. Sigbjarnarson (Ed.), The Water and the Land, National Energy Authority, Reykjavik, 1990, pp. 121–128.
[31] H. Tomasson, Glacial and volcanic shore interactions, Part I: on land, in: G. Sigbjarnarson (Ed.), Iceland Coastal and River Symposium, 1986, pp. 7–16, Reykjavik.
[32] M. Meybeck, How to establish and use world budgets of riverine materials, in: A. Lerman, M. Meybeck (Eds.), Physical and Chemical Weathering in Geochemical Cycles, Kluwer Academic Publishers, 1988, pp. 247–272.
[33] S.R. Gislason, E.S. Eiriksdottir, B. Sigfusson, A. Snorrason, S.O. Elefsen, J. Hardardottir, M.I. Kardjilov, E.H. Oelkers, P. Torsander, G. Gisladottir, N.O. Oskarsson, The effect of climate, vegetation, rock age, and human activity on basalt weathering rates in NE-Iceland, Geochim. Cosmochim. Acta 69 (10) (2005) A681–A681.
[34] P. van Calsteren, J.B. Schwieters, Performance of a thermal ionization mass-spectrometer with a deceleration lens system and post-deceleration detector selection, Int. J. Mass Spectrom. Ion Process. 146 (1995) 119–129.
[35] S. Turner, P. van Calsteren, N. Vigier, L. Thomas, Determination of thorium and uranium isotope ratios in low-concentration geological materials using a fixed multi-collector-ICP-MS, J. Anal. At. Spectrom. 16 (6) (2001) 612–615.
[36] R.H. James, M.R. Palmer, The lithium isotope composition of international rock standards, Chem. Geol. 166 (3–4) (2000) 319–326.
[37] G.D. Flesch, A.R. Anderson, H.J. Svec, A secondary isotopic standard for $^6Li/^7Li$ determinations, Int. J. Mass Spectrom. Ion Process. 12 (1973) 265–272.
[38] N. Vigier, K.W. Burton, S.R. Gislason, N.W. Rogers, S. Duchene, L.E. Thomas, E. Hodge, B.F. Schaefer, The relationship between riverine U-series disequilibria and erosion rates in a basaltic terrain, Earth Planet. Sci. Lett. (in press).
[39] S.R. Gislason, M.I. Kardjilov, G. Gisladottir, E.S. Eiriksdottir, B. Sigfusson, S. Elefsen, A. Snorrason, D. Wolff-Boenisch, E. Oelkers, P. Torsander, A quantitative field based study of basalt/basaltic glass weathering and its role in carbon fixation, Geochim. Cosmochim. Acta 66 (15A) (2002) A275–A275.
[40] O. Sigmarsson, Short magma chamber residence time at an Icelandic volcano inferred from U-series disequilibria, Nature 382 (6590) (1996) 440–442.
[41] O. Sigmarsson, C. Hemond, M. Condomines, S. Fourcade, N. Oskarsson, Origin of silicic magma in Iceland revealed by Th isotopes, Geology 19 (6) (1991) 621–624.
[42] P. Louvat, C.J. Allegre, Present denudation rates on the island of reunion determined by river geochemistry: basalt weathering and mass budget between chemical and mechanical erosions, Geochim. Cosmochim. Acta 61 (17) (1997) 3645–3669.
[43] Y. Smit, The Snaefellsnes Transect: A geochemical cross-section through the Iceland Plume, PhD, The Open Univeristy, 2001.
[44] S.R. Gislason, S. Arnorsson, Saturation state of natural waters in Iceland relative to primary and secondary minerals in basalts, in: Fluid–Mineral Interactions: A Tribute to H.P. Eugster, R.J. Spencer, M. Chou, eds., Geochemical Society, Special Publication 2, pp. 373–393, 1990.
[45] D.L. Parkhurst, C.A.J. Appelo, User's guide to PHREEQC (version 2) — a computer program for speciation, batch-reaction, one-dimensional transport, and inverse geochemical calculations, Water-Resouces Investigations, 1999.

[46] J. Riotte, F. Chabaux, (U-234/U-238) activity ratios in freshwaters as tracers of hydrological processes: the Strengbach watershed (Vosges, France), Geochim. Cosmochim. Acta 63 (9) (1999) 1263–1275.
[47] D. Langmuir, Aqueous Environmental Geochemistry, Prentice-Hall, 1997.
[48] J. Kronfeld, J.C. Vogel, Uranium isotopes in surface waters from Southern Africa, Earth Planet. Sci. Lett. 105 (1–3) (1991) 191–195.
[49] P.A.E. Pogge von Strandmann, K.W. Burton, R.H. James, P. Van Calsteren, S.R. Gislason, The behaviour of non-traditional light and uranium isotopes in climatically varied basaltic estuaries, Earth Planet. Sci. Lett. (in preparation).
[50] P.B. Tomascak, Developments in the understanding and application of lithium isotopes in the earth and planetary sciences, Geochemistry of Non-Traditional Stable Isotopes, Reviews in Mineralogy and Geochemistry, vol. 55, 2004, pp. 153–195.
[51] T. Magna, U.H. Wiechert, D. Harrison, A.N. Halliday, F.M. Stuart, Combined Li and He isotopes in iceland and Jan Mayen Island lavas and the nature of the North Atlantic mantle, Earth Planet. Sci. Lett. (in review).